

Thermo- and pH-Responsive Hydrogel-Coated Gold Nanoparticles

Jun-Hyun Kim and T. Randall Lee*

Department of Chemistry, University of Houston, 4800 Calhoun Road,
Houston, Texas 77204-5003

Received February 15, 2004. Revised Manuscript Received June 3, 2004

This article describes the structural and optical properties of a new class of hybrid nanoparticles that consists of a small gold core (~60 nm in diameter) coated with a biocompatible hydrogel polymer shell varying from ~20 to ~90 nm in thickness. These nanoparticles are being developed to serve as unique drug-delivery vehicles that have the ability to respond to ambient changes in pH and/or temperature. A particularly attractive feature of these nanoparticles derives from the fact that the hydrogel can be thermally activated by exposure to light via exploitation of the strong plasmon absorption of the gold nanoparticle core. The hydrogel coating consists of a known biocompatible thermo-responsive copolymer derived from the radical polymerization of a selected mixture of *N*-isopropylacrylamide and acrylic acid. The morphology and elemental composition of the composite nanoparticles were characterized by field emission scanning electron microscopy and energy-dispersive X-ray scattering, respectively. The optical properties of the nanoparticles were analyzed by UV spectroscopy, and the average particle size was evaluated as a function of temperature and/or pH using dynamic light scattering. The results demonstrate not only that these new hybrid nanoparticles can be reliably prepared through the surfactant-free emulsion polymerization but also that their responses to external stimuli are completely consistent with the targeted drug-delivery objectives.

Introduction

In recent years, colloidal scientists have shifted the focus of their research from micrometer-sized particles to nanometer-sized particles. In particular, studies of inorganic nanostructured materials have received much attention due to their unique optical properties and biocompatible characteristics.¹ Nevertheless, significant new advances in the fabrication of nanoparticles are needed to further the development of nanoscale tools and devices. Metal nanoparticles, in particular, can be superior to molecular chromophores due to their ability to adsorb and/or scatter light.² Many researchers have demonstrated the use of platinum,³ silver,⁴ and copper,⁵ and particularly gold⁶ as nanoparticle-based optical materials.

Given their biocompatible nature and unique optical properties, gold nanoparticles are particularly attractive as components in photothermally responsive biomaterials. Indeed, a specific goal of our research is to develop discrete hydrogel-coated gold nanoparticles that exhibit structural changes upon exposure to light. Hydrogels play key roles in a variety of technological applications,⁷

including drug delivery, chemical separations, and catalysis.^{8,9} The hydrogels of interest to us are cross-linked polymer particles that can be dispersed as colloids in aqueous solution. These hydrogels readily undergo volume changes that are strongly dependent on the lower critical solution temperature (LCST)^{10,11} as well as other chemical or physical circumstances, such as the solution pH and the nature of the solvent.¹² Meanwhile, numerous thermo- and pH-responsive shell/core particles have been developed to modify a specific physical property of the particles or to impart thermo-responsiveness to otherwise unresponsive particles.¹³ As a consequence, hydrogel-based particles have the potential for use in a variety of applications (e.g., enhanced oil recovery, controlled reversible flocculation, and the uptake and release of heavy metals).¹⁴

Thermo-sensitive hydrogels based on poly(*N*-isopropylacrylamide) (NIPAM) have been particularly well studied.^{7,15–17} It is known that hydrogels based on the

* To whom correspondence should be addressed.

(1) Kreibig, U.; Vollmer, M. *Optical Properties of Metal Clusters*; Springer Series in Material Science; Springer: Berlin, 1995; Vol. 25.

(2) Bohren, C. F.; Hoffman, D. R. *Absorption and Scattering of Light by Small Particles*; Wiley: New York, 1998.

(3) Teranishi, T.; Miyake, M. *Chem. Mater.* **1998**, *10*, 594.

(4) Quaroni, L.; Chumanov, G. *J. Am. Chem. Soc.* **1999**, *121*, 10642.

(5) Chen, S.; Sommers, J. M. *J. Phys. Chem. B* **2001**, *105*, 8816.

(6) Clark, H. A.; Campagnok, P. J.; Wuskell, J. P.; Lewis, A.; Loew, L. M. *J. Am. Chem. Soc.* **2000**, *122*, 10234.

(7) Pelton, R. *Adv. Colloid Interface Sci.* **2000**, *85*, 1.

(8) Jeong, B.; Bae, Y. H.; Lee, D. S.; Kim, S. W. *Nature* **1997**, *388*, 860.

(9) Bergbreiter, D. E.; Case, B. L.; Liu, Y. S.; Caraway, J. W. *Macromolecules* **1998**, *31*, 6053.

(10) Schild, H. G.; Tirrell, D. A. *J. Phys. Chem.* **1990**, *94*, 4352.

(11) Saunders, B. R.; Vincent, B. *J. Chem. Soc., Faraday Trans.* **1996**, *92*, 3385.

(12) Zhou, S.; Chu, B. *J. Phys. Chem. B* **1998**, *102*, 1364.

(13) Jones, C. D.; Lyon, L. A. *Macromolecules* **2000**, *33*, 8301.

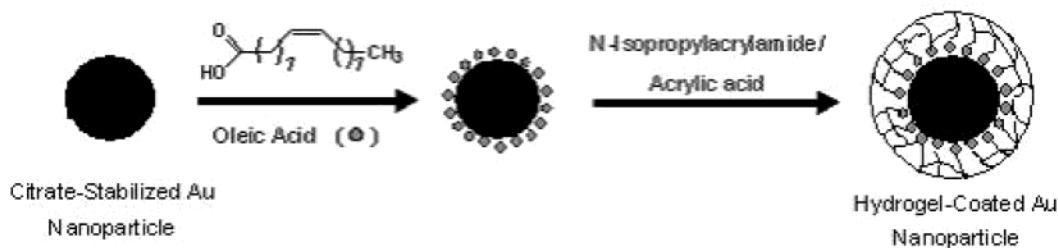
(14) Snowden, M. J.; Tomas, D.; Vincent, B. *Analyst* **1993**, *118*, 1367.

(15) Jones, C. D.; Lyon, L. A. *Macromolecules* **2003**, *36*, 1988.

(16) Mears, S. J.; Deng, Y.; Cosgrove, T.; Pelton, R. *Langmuir* **1997**, *13*, 1901.

(17) Zhu, M. Q.; Wang, L. Q.; Exarhos, G. J.; Li, A. D. Q. *J. Am. Chem. Soc.* **2004**, *126*, 2656.

Scheme 1. Hydrogel Growth on Gold Nanoparticle Using Surfactant-Free Emulsion Polymerization (SFEP)



homo-polymer NIPAM are limited in their applications because this material undergoes a thermally induced conformational change at a fixed LCST of 32 °C.¹⁸ Researchers have overcome this limitation by introducing acrylic acid (AAc) into the polymer backbone, which can shift the LCST of the copolymer anywhere from 32 to 60 °C.¹⁹ The presence of AAc in the poly-NIPAM bulk particles not only increases the LCST but also causes the particle to undergo a discontinuous transition and a large change in volume. The material is highly water-swollen below the LCST, but becomes partially desolvated, depending on the details of the polymer structure, when heated above its LCST. These hydrogels undergo a completely reversible swelling–collapsing transition in response to changes in both temperature and pH.

In this work, we utilize surfactant-free emulsion polymerization (SFEP)^{20–25} to encapsulate gold nanoparticles within larger spherical hydrogel particles (Scheme 1). This approach produces a stable, compact, and chemically resistant polymer overlayer. It also can be used to coat organic and inorganic particles on the micrometer and submicrometer scales.¹ Our long-range goal of this research is to prepare thermo- and pH-responsive hydrogel copolymer-coated gold nanoparticles that can be photolytically activated. This report describes the preparation and characterization of the first-generation species in which conformational changes lead to alternations in the release profile of entrapped water in response to changes in temperature and pH.²⁶

Experimental Section

Materials. The monomer *N*-isopropylacrylamide (NIPAM) was obtained from Acros (99%), recrystallized in hexane, and dried under vacuum before use. Acrylic acid (AAc, Acros, 99.5%), potassium hydroxide (KOH, EM, 85%), nitric acid (HNO₃, EM, 70%), ammonium persulfate (APS, EM, 98%), and oleic acid (OA, J. T. Baker) were all used as received from the indicated suppliers. Water used in all reactions, solution preparations, and polymer isolations was purified to a resistance of 10 MΩ (Milli-Q Reagent Water System, Millipore

Corporation) and filtered through a 0.2 μm filter to remove any particulate matter. In the preparation of gold nanoparticles, trisodium citrate (EM, 99%) and hydrogen tetrachloroaurate (Strem, Au 99.9%) were used without purification.

Preparation of Gold Nanoparticles. Gold nanoparticles were prepared via the common technique of citrate reduction, which has been described in detail.^{27–29} The sizes of our gold nanoparticles were always between 55 and 65 nm as judged by dynamic light scattering (DLS) and field emission scanning electron microscopy (FE-SEM). The glassware was cleaned first with strong acid (3/1 HCl/HNO₃) and then with strong base (saturated KOH in isopropyl alcohol) before use.

Synthesis of Hydrogel-Coated Gold Nanoparticles. The hydrogel-coated gold nanoparticles were prepared by SFEP in aqueous solution. In a three-necked round-bottomed flask equipped with a reflux condenser and an inlet for argon gas, gold colloidal solutions were diluted with purified Milli-Q water to give a maximum of ~0.25 au at 530 nm. The solution was purged with argon for 1 h and was bubbled through the solution for the duration of the reaction to remove any oxygen, which can intercept radicals and disrupt the polymerization. The solution was agitated using a football-shaped Teflon-coated magnetic stirring bar. Degassed oleic acid (1.6 mL, 0.001 M), which has a low affinity toward gold, was then added to the stock solution under argon. The mixture was stirred for 1 h and placed in an ultrasonicator for 15 min. An approximately 94:6 wt % ratio of NIPAM (26.1 mL, 0.01 M): AAc (1.6 mL, 0.01 M) was then added and stirred for 15 min to give homogeneity. The solution was then heated to 71 °C in an oil bath, and then APS (0.8 mL, 0.01 M) was added to initiate the polymerization. The reaction time, which depended on the amount of starting materials, was varied between 6 and 8 h. At the end of this period, the solution was cooled and filtered through a 1 μm membrane to remove any micrometer-sized impurities and/or any aggregated particles. The filtered solution was centrifuged at 20 °C for 2 h at 3500 rpm with RC-3B Refrigerated Centrifuge (Sorvall Instruments), and the supernatant was separated to remove unreacted materials, soluble side products, and seeds of pure polymer. The purified nanoparticles were then diluted with pure Milli-Q water and stored at room temperature for later use. The size of the hydrogel-coated gold particles could be varied between 100 and 230 nm by controlling the amount of monomer and initiator as well as the reaction time.

Characterization of Gold and Hydrogel-Coated Gold Nanoparticles. To characterize the pure gold nanoparticles and hydrogel-coated gold nanoparticles, we used field emission scanning electron microscopy (FE-SEM), energy dispersive X-ray (EDX) analysis, ultraviolet–visible (UV–vis) spectroscopy, and dynamic light scattering (DLS). Due to our interest in thick hydrogel coatings, our most thorough analyses were focused on the hydrogel-coated gold nanoparticles having ~230-nm diameters.

(18) Pelton, R. H.; Pelton, H. M.; Morphesis, A.; Rowell, R. L. *Langmuir* **1989**, *5*, 816.

(19) Snowden, M. J.; Chowdhry, B. Z.; Vincent, B.; Morris, G. E. *J. Chem. Soc., Faraday Trans.* **1996**, *92*, 5013.

(20) Saunders, B. R.; Vincent, B. *Adv. Colloid Interface Sci.* **1999**, *80*, 1.

(21) Sunders, B. R.; Crowther, H. M.; Vincent, B. *Macromolecules* **1997**, *30*, 482.

(22) Kawaguchi, H.; Fujimoto, K.; Mizuhara, Y. *Colloid Polym. Sci.* **1992**, *270*, 53.

(23) Corpart, J. M.; Candau, F. *Colloid Polym. Sci.* **1993**, *271*, 1055.

(24) Neyret, S.; Vincent, B. *Polymer* **1997**, *38*, 6129.

(25) Olekiminta, D. H.; Luckham, P. F. *Polymer* **1995**, *36*, 4827.

(26) Sershon, S. R.; Westcott, S. L.; Halas, N. J.; West, J. L. *J. Biomed. Mater. Res.* **2000**, *51*, 293.

(27) Frens, G. *Nature Phys. Sci.* **1973**, *241*, 20.

(28) Turkevich, J.; Stevenson, P. C.; Hillier, J. *Discuss. Faraday Soc.* **1951**, *58*, 55.

(29) Goodman, S. L.; Hodges, G. H.; Trejdosiewicz, L. K.; Linvinton, D. C. *J. Microsc.* **1981**, *123*, 201.

We employed a Cary 50 Scan UV–vis optical spectrometer (Varian) with Cary Win UV software to characterize the optical properties of the bare gold nanoparticles and the hydrogel-coated gold nanoparticles. UV–vis spectra of the prepared gold nanoparticles were collected by diluting the particles with Milli-Q water, transferring them to an optical glass cell, and scanning over a range of wavelengths (400–1100 nm). The hydrogel-coated gold nanoparticles were analyzed as prepared (i.e., without dilution). For consistency, UV–vis spectra of the distinct batches of nanoparticles were collected both before and after coating with the hydrogel.

Analysis by FE-SEM was performed using a JSM 6330F (JEOL) instrument operating at 15 kV and equipped with a setup for elemental analysis by EDX (Link ISIS software series 300, Oxford Instruments). To collect both FE-SEM images and EDX data, the gold nanoparticles and hydrogel-coated nanoparticles were deposited on Formvar-coated copper grids and completely dried at room temperature overnight prior to analysis. The samples were then coated with a carbon film (2.5 nm thick) using a vacuum sputterer. The gold and hydrogel-coated gold nanoparticles were examined by FE-SEM (magnification 20–100 K) to demonstrate the overall morphological uniformity of the particles and by EDX to confirm the presence of the gold nanoparticle core.

For the DLS measurements, an ALV-5000 Multiple Tau Digital Correlation instrument operating at a light source wavelength of 514.5 nm and a fixed scattering angle of 90° was used to measure particle size as a function of temperature and pH for gold and hydrogel-coated gold nanoparticles. The samples were measured at dilute concentrations with precise control over the temperature (especially at higher temperatures to reduce artifacts resulting from convection currents in the samples). For all samples, data were collected from 20 to 60 °C. All data showed good Gaussian distribution curves, and the standard deviation of the distribution was 5 to 20% of the mean for all samples.

Results and Discussion

We used SFEP at 71 °C in aqueous solution to prepare the hydrogel-coated gold nanoparticles. This method was found to be convenient and reliable; moreover, all starting materials and products were soluble under the reaction conditions, which circumvented the need for purification during the reaction. A disadvantage of this technique, however, is that phase separation can occur if the reaction conditions (e.g., reaction time, stirring speed, temperature, or concentration of monomers) are varied widely. Using this approach, we were able to prepare hydrogel-coated gold nanoparticles as stable colloids with gold cores having ~60 nm diameters and shell thicknesses varying from ~20 to 90 nm. These composite particles remained stable for more than 2 months at room temperature. Furthermore, particles with thin hydrogel coatings were more reliably produced than those with thick hydrogel coatings. Specifically, thinly coated particles (shell thickness ≤ 50 nm) were produced without failure, while those with the thickest coatings (≥ 60 nm) were cleanly produced only about one-third of the time, with the contaminant being discrete hydrogel particles having no gold center.³⁰

Figure 1a presents the UV–vis absorption spectra of the bare and hydrogel-coated gold nanoparticles, which shows a maximum absorption band at 530–540 nm arising from the gold plasmon.³¹ The presence of the asymmetric band centered at 535 nm is consistent with the formation of spherical particles.³² Indeed, a homo-

(30) Preliminary studies in our laboratory have shown, however, that the particles with gold cores can be separated from those without gold cores using density-fractionation centrifugation.

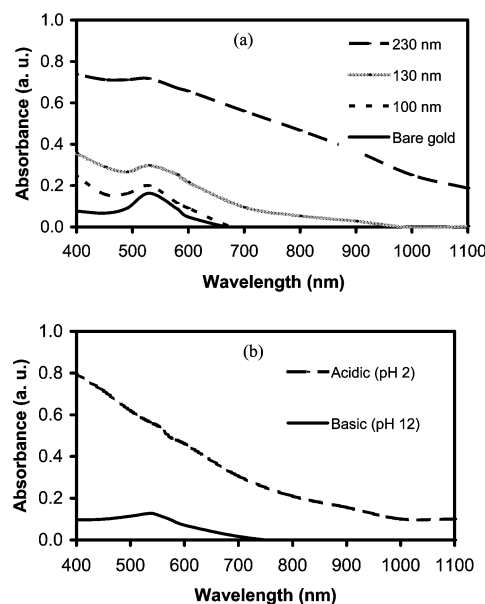


Figure 1. UV–visible spectra of bare gold nanoparticles (60 nm) and hydrogel-coated gold nanoparticles of varying size (a) under neutral conditions and (b) as a function of pH for 230 nm composite particles.

geneous distribution of spherical gold nanoparticles was confirmed by the FE-SEM images (see below). The position of the plasmon band is sensitive to particle size and shape as well as to the optical and electronic properties of the particle surroundings.³³ The UV–vis spectra of solutions of hydrogel-coated gold nanoparticles are similar to those of silica-coated gold nanoparticles.³⁴ When the thickness of the hydrogel coating increases (Figure 1a), the gold plasmon band decreases in intensity. The decrease in intensity arises because the refractive index of the copolymer is different from that of water and that of the gold nanoparticles, which leads to an increase in UV scattering with increasing hydrogel thickness. There is, however, no readily discernible shift of the plasmon absorption maximum. For the thicker coatings, scattering appears to dominate at shorter wavelengths, leading to an apparent weakening of the plasmon band. The behavior is consistent with the work of Aden and Kerker,³⁵ which represents a modification of Mie theory³⁶ for shell/core particles.

To examine the particle diameter as a function of pH, we adjusted the pH of aqueous hydrogel-coated gold nanoparticle solutions by adding small quantities of dust-free aqueous solution of either 0.01 M HCl or 0.01 M KOH. Figure 1b shows the pH dependence of the UV–vis spectra, which illustrate the broad increase in the extinction band intensity with decreasing pH. This phenomenon arises from the swelling–collapsing properties of the hydrogel coating. At high pH, the hydrogel is water-swollen due to charge–charge repulsion, and one observes predominantly absorption due to the gold core. Under acidic conditions, however, the diameter of

(31) Link, S.; El-Sayed, M. A. *J. Phys. Chem. B* **1999**, *103*, 4212.
 (32) Rivas, L.; Sanchez-Cortes, L.; Garcia-Ramos, J. V.; Morcillo, G. *Langmuir* **2001**, *17*, 574.
 (33) Underwood, S.; Mulvaney, P. *Langmuir* **1994**, *10*, 3427.
 (34) Liz-Marzan, L. M.; Giersig, M.; Mulvaney, P. *Langmuir* **1996**, *12*, 4329.
 (35) Aden, A. L.; Kerker, M. *J. Appl. Phys.* **1951**, *22*, 1242.
 (36) Mie, G. *Ann. Phys. (Leipzig)* **1908**, *25*, 377.

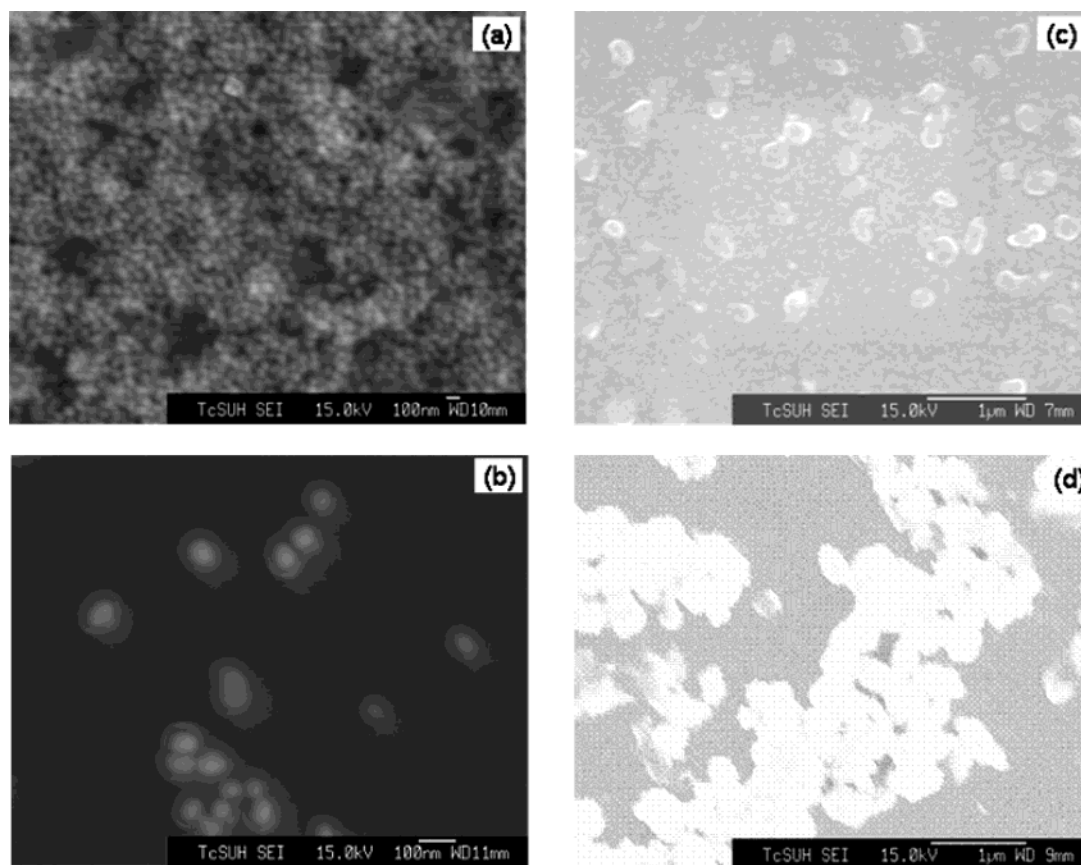


Figure 2. FE-SEM micrographs of (a) bare gold nanoparticles (~ 60 nm) and (b–d) hydrogel-coated 60 nm gold nanoparticles with varying overall diameter: (b) ~ 100 nm, (c) ~ 130 nm, and (d) ~ 230 nm.

the hydrogel-coated gold nanoparticles shrink, and one observes predominantly scattering due to the hydrogel-rich phase of the polymer, which densely coats the gold nanoparticle surface. This swelling and collapsing phenomenon was also readily observed visually as characterized by color changes of the particle solution (hot pink at high pH and milky white at low pH).

Figure 2 shows the FE-SEM micrographs of the gold nanoparticle cores and of hydrogel-coated gold nanoparticles having composite diameters. Analysis by FE-SEM has advantages over conventional SEM because the relatively high current density confined within a small beam diameter affords an increase in resolution.³⁷ The micrographs show that all of the gold nanoparticle cores are spherical, but the hydrogel-coated nanoparticles are somewhat inhomogeneously shaped, particularly for those having thicker coatings. Indeed, we have found that the use of a surfactant in the polymerization reaction affords smoother surfaces but thinner coatings. The surfaces of the gold particles appear to be completely coated given the absence of gold-core images among the hydrogel particles.

The EDX spectra were obtained from the same two-dimensional raft of hydrogel-coated gold nanoparticles. Figure 3 provides a representative spectrum of the 230 nm hydrogel-coated nanoparticles, which shows the presence of peaks characteristic of gold at 2.12 and 9.71 keV. Peaks due to copper are also present, but these arise due to X-ray emission from the supporting grid.

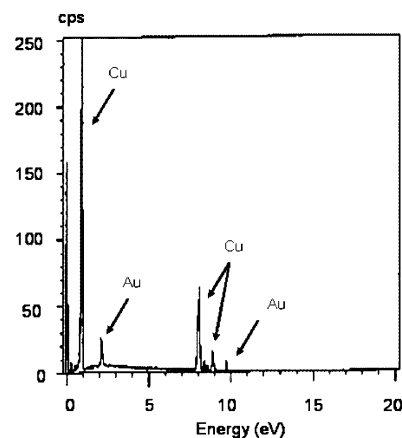


Figure 3. EDX spectrum of hydrogel-coated gold nanoparticles (230 nm diameter).

The intensities of the gold peaks for hydrogel-coated nanoparticles are much weaker than those for bare gold nanoparticles collected at the same energy level (data not shown). Furthermore, analogous hydrogel particles grown without a gold core showed only the presence of copper (due to the grid); these data therefore collectively confirm the synthesis of hydrogel-coated gold nanoparticles.

Using DLS, we observed an increase in the diameter of the ~ 230 nm hydrogel-coated and gold nanoparticles with increasing pH (Figure 4). Bare gold nanoparticles exhibited no similar pH-dependent behavior, but the hydrogel-coated gold nanoparticles showed a diameter change of ~ 60 nm. The pH range for the swelling transition of the hydrogel-coated gold nanoparticles

(37) Grabar, K. C.; Brown, K. R.; Keating, C. D.; Stranick, S. J.; Tang, S.; Natan, M. J. *Anal. Chem.* **1997**, *69*, 471.

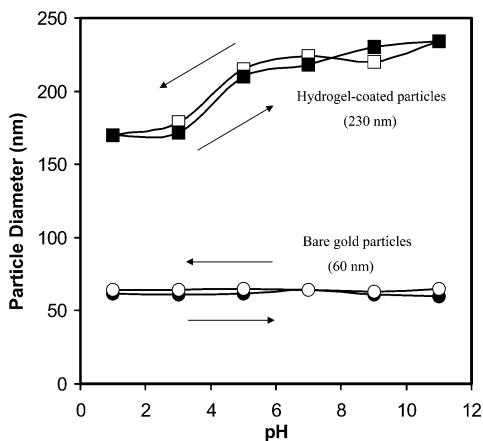


Figure 4. Hydrodynamic diameter of bare gold and hydrogel-coated gold nanoparticles as a function of pH. Filled symbols correspond to increasing pH; open symbols correspond to decreasing pH.

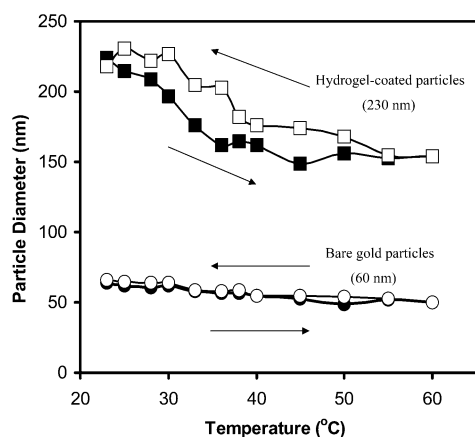


Figure 5. Hydrodynamic diameter of bare gold and hydrogel-coated gold nanoparticles as a function of temperature. Filled symbols correspond to increasing temperature; open symbols correspond to decreasing temperature.

occurs between pH 3 and pH 6, which is consistent with the known pK_a value for acrylic acid (4.25).³⁸ Under acidic conditions, the particles shrink due to neutralization of the carboxylate groups. Under alkaline conditions, however, the particles are expanded due to internal electrostatic repulsion among anionic carboxylate groups. The gradual rather than abrupt increase in the observed swelling behavior can perhaps be attributed to an inhomogeneous distribution of ionizable groups.³⁸

Figure 5 shows the hydrodynamic diameter of the hydrogel-coated and bare gold nanoparticles in dilute neutral solution as a function of temperature. The diameter of the hydrogel-coated gold nanoparticles decreases with increasing temperature, while the diameters of the bare gold nanoparticles remain constant. Collapse of the hydrogel at elevated temperatures likely arises from the loss of hydrogen bonding to hydrophilic sites ($-C=O$, $-NH$) in the hydrogel copolymer.³⁹ The thermally induced loss of hydrogen bonding removes internal electrostatic repulsion within the hydrogel matrix, leading to a collapse of the swelled structure.³⁹

The electrostatic environment can be adjusted by introducing ionizable groups along the polymer backbone (e.g., acrylic acid moieties). The presence of water molecules and hydrophilic sites gives rise to hydrogen-bonding interactions at low temperatures, allowing electrostatic repulsion to enhance the water-swelling behavior.⁴⁰

The LCST of pure *N*-isopropylacrylamide hydrogels is ~ 32 °C,⁴¹ but our hydrogel-coated gold nanoparticles contain 6% acrylic acid, which should, in principle, increase the LCST to ~ 34 °C.³⁸ Figure 5 shows, however, that as the temperature was increased above 30 °C, the particle size decreased gradually and became constant above 45 °C. We propose that the change in the polymer backbone of NIPAM-*co*-AAc polymer-coated gold nanoparticles decreases the average interchain distance in the polymer and thereby increases and broadens the LCST in our system.

In separate studies, we found that heating NIPAM-*co*-AAc particles having no gold cores led to a decrease in the hydrodynamic diameter by a factor of 2, which corresponds to an 8-fold decrease in the effective particle volume.⁴² In contrast, the hydrogel-coated nanoparticles exhibited a decrease in overlayer thickness of only 30%, which corresponds to an approximately 3-fold decrease in the effective volume of the hydrogel coat. We also found that temperature induces a greater change in the diameter of hydrogel-coated gold nanoparticles than does pH, which suggests that the particle-swelling behavior is dominated more by the NIPAM component than the pH-dependent size changes effected by the AAC component.

Conclusions

This work has demonstrated the effective encapsulation of gold nanoparticles within a biocompatible hydrogel overlayer. Typically, the gold cores were ~ 60 nm in diameter, and the thickness of the hydrogel overlayer varied from 20 to 90 nm. The morphology, elemental composition, and properties of the composite nanoparticles were characterized by UV-vis spectroscopy, FE-SEM, and EDX. These data collectively support the formation of discrete hydrogel-coated gold nanoparticle cores. Analysis by DLS revealed morphological changes that occurred in response to variations in temperature and pH; specifically, the diameters of the hydrogel-coated gold nanoparticles were observed to decrease with increasing temperature and decreasing pH. As a whole, the results demonstrate that these hybrid nanoparticles can be readily prepared through the SFEP method and that their responses to changes in temperature and pH are consistent with their ultimate use as drug-delivery vehicles.

Acknowledgment. We gratefully acknowledge financial support from the Army Research Office and the Robert A. Welch Foundation (Grant E-1320). We also thank Dr. J. K. Meen for assistance with the FE-SEM measurements and Dr. J. C. Reina for assistance with the DLS measurements.

CM049764U

(38) Morris, G. E.; Vincent, B.; Snowden, M. J. *J. Colloid Interface Sci.* **1997**, *190*, 198.

(39) Shibayama, M.; Mizutani, S.; Nomura, S. *Macromolecules* **1996**, *29*, 2019.

(40) Kato, E. *J. Chem. Phys.* **1997**, *106*, 3792.

(41) Tan, K. C.; Wu, X. Y.; Pelton, R. H. *Polymer* **1992**, *33*, 436.

(42) Tan, K. C.; Ragaram, S.; Pelton, R. H. *Langmuir* **1994**, *10*, 418.